Effects of Beam Misalignment on Heterogeneous Cellular Networks with Mm-Wave Small Cells

Muhammad Saad Zia, Douglas M. Blough and Mary Ann Weitnauer
School of Electrical and Computer Engineering
Georgia Institute of Technology, Atlanta, Georgia 30332-0250, USA
Email: saad.zia@gatech.edu; doug.blough@ece.gatech.edu; mary.ann.weitnauer@ece.gatech.edu

GLOBECOM 2022 - 2022 IEEE Global Communications Conference | 978-1-6654-3540-6/22/$31.00 ©2022 IEEE | DOI: 10.1109/GLOBECOM48099.2022.10001400

***Abstract*—This paper studies the effects of millimeter-wave (mm-wave) beam alignment errors on the downlink achievable rate of a heterogeneous network (HetNet), which consists of sub-6 GHz macro-cells and mm-wave small-cells. The alignment error is modeled as a function of the underlying mm-wave link parameters. The conventional maximum biased received power criterion, where the bias is used for mm-wave small-cells, is adopted for cell associations. By varying the value of the bias factor, we investigate the changes in the downlink rate coverage probability. Our simulation results indicate that high values (of the order of 30 dB) for the bias, while beneficial in the case of perfect alignment, are actually disadvantageous for the low-rate users in the case of imperfect beam alignment. The low-rate users are better served by a moderate value (of the order of 20 dB) of the bias when the beam alignment errors are accounted for. We also show that the above disparity can be narrowed down by increasing by mm-wave base station (BS) antennas and/or the mm-wave BS density.**

***Index Terms*—Beam alignment error, bias, HetNet, non line-of-sight, rate coverage probability.**

I. Introduction

The bandwidth that the millimeter-wave (mm-wave) frequencies can offer is unparalleled in the traditionally used sub-6 GHz band [1]–[3]. However, it is widely accepted that a stand-alone deployment of mm-wave networks is rather unrealistic because of the anticipated outages stemming from the unique propagation characteristics of mm-wave frequencies, such as the extreme sensitivity to blockages [4]–[7]. Therefore, a more practical scenario is the coexistence of the mm-wave small-cells with the sub-6 GHz macro-cells, thus, giving rise to heterogeneous networks (HetNets) that can provide extremely high data rates and avoid outages [5]–[9].

The path-loss at mm-wave frequencies is extremely high, which necessitates the use of antenna arrays along with beamforming [10]. For effective beamforming at mm-wave frequencies, channel estimation is required [11]. However, inherent limitations of channel estimation result in beam alignment errors, which reduce the beamforming gain and degrade the system performance [12]. It is, therefore, extremely important to investigate the impacts of mm-wave beam alignment errors on the achievable rates of HetNets.

In the existing literature, beam alignment errors have been studied mostly in the context of mm-wave only networks, e.g., [12]–[14]. The works in [15] and [16] analyze beam alignment errors for multiple tiers of mm-wave base stations (BSs), but the dependence of the alignment error on the link parameters is ignored.

In [5], [6] and [8], the concept of downlink-uplink decoupling in HetNets is investigated. The cell associations are decided according to the maximum biased received power criterion, where a bias factor is used to offload user equipments (UEs) from the sub-6 GHz macro-cells to the mm-wave small-cells. In [9], small-cells operating on both the frequency bands are considered in addition to sub-6 GHz macro-cells and two bias factors are used to optimize the network performance. A generalized user association scheme is proposed in [7] and it is shown that simultaneously maximizing the signal-to-interference-plus-noise ratio (SINR) coverage and the link rate is not possible when the macro-cells and the small-cells operate on different frequency bands. The aforementioned works on dual-band HetNets, however, assume perfect alignment between the UEs and their serving mm-wave BSs. To the best of the authors' knowledge, no prior work addresses how the performance of such HetNets is impacted in the presence of beam alignment errors, which depend on the link parameters.

This paper investigates the impact of mm-wave beam misalignment on the downlink rate coverage probability of a HetNet consisting of sub-6 GHz and mm-wave BSs. The conventional maximum biased received power criterion is used for cell associations. The beam alignment error is formulated as a function of the mm-wave link parameters similar to our previous work [13]. The work in [13], however, focused on a mm-wave only network. Our simulation results in this paper illustrate that aggressive biasing (of the order of 30 dB) towards the mm-wave BSs, while beneficial for high-rate UEs, is actually detrimental for low-rate UEs when the beam alignment errors are accounted for. Such an observation about the impact of beam alignment errors has not been reported before and constitutes the novelty of this work.

II. System Model

This paper considers the downlink of a two-tier heterogeneous cellular network (HetNet). The first tier consists of the macro-cell base stations (BSs) operating on sub-6 GHz frequencies whereas the second tier comprises small-cell BSs operating on the mm-wave frequencies. The locations of the BSs in each tier are modeled as an independent homogeneous Poisson point process (PPP) in the two-dimensional plane, $\mathbb{R}^2$. The PPPs for Tier 1 and Tier 2 BS locations are represented as

Φ_m and Φ_s, respectively and the corresponding intensities are given by λ_m and λ_s. Tier 1 differs from Tier 2 in terms of the downlink transmit power, spatial density, and the propagation characteristics [6]. The downlink transmit powers of Tier 1 and Tier 2 BSs are represented by the constants P_m and P_s, respectively, where $P_m > P_s$. Throughout the rest of the paper, the subscripts m and s are used to specify the sub-6 GHz and the mm-wave tiers, respectively.

The user equipment (UE) locations are assumed to follow another independent homogeneous PPP, Φ_u, with intensity λ_u. Each UE transmits with a constant power level P_u. Moreover, each UE is assumed to operate on both the sub-6 GHz and the mm-wave bands [9]. As per the convention of stochastic geometric analysis, it is assumed that a *typical* UE is stationed at the origin and the analysis is performed on this typical UE [17]. The BS that serves the typical UE is labelled as the tagged BS. Let the location of the tagged BS be denoted by x^*. The length, r, of the link between the tagged BS and the typical UE is written as $r = \|x^*\|$.

The blockage effects for the mm-wave tier are emulated using the generalized LOS ball blockage model of [2], which approximates the irregularly shaped LOS region around the UE/BS under consideration by a disk of a specific fixed radius, R_B. If the link length r from/to the considered node is such that $r \leq R_B$, then the link is either LOS with probability $\mathcal{P}_{LOS}$, or NLOS with probability $\mathcal{P}_{NLOS} = 1 - \mathcal{P}_{LOS}$. If $r > R_B$, then the link can only be NLOS.

To model the path-loss for the sub-6 GHz and the mm-wave links, we adopt the floating-intercept path-loss model of [6]:

$$L_j(r) = C_j r^{-\alpha_j}, \tag{1}$$

where α_j and C_j are the empirical path-loss parameters [3]. The path-loss experienced by the LOS mm-wave links is different from that experienced by the corresponding NLOS links [1], therefore $j \in \{m, LOS, NLOS\}$.

We assume independent small-scale fading for each link. The fading for the mm-wave links is modeled using the Nakagami distribution, where Nakagami shape parameters N_{LOS} and N_{NLOS} are used for the LOS and the NLOS states, respectively, such that $N_{\text{LOS}} = 3$ and $N_{\text{NLOS}} = 2$ [4], [12]. Since sub-6 GHz channels exhibit rich scattering as compared to the mm-wave channels, we assume independent and identically distributed Rayleigh fading for the sub-6 GHz links.

We assume that the network is two dimensional and we consider that beamforming is performed by the mm-wave BSs only in the horizontal plane while the elevation angle is kept constant at $\frac{\pi}{2}$. We consider that antenna arrays are utilized at the mm-wave BSs whereas each sub-6 GHz BS utilizes a single omni-directional antenna for its transmissions [5], [6]. The antenna gain, G_m, of a sub-6 GHz BS is assumed to be 3 dBi [1] [15]. At the UE side, a single isotropic antenna is considered with a 0 dBi gain. For the mm-wave tier, we further consider three sectors at each mm-wave BS, where each sector, covering $120°$, makes use of a uniform linear array (ULA) composed of M directional antenna elements [13]. Moreover, analog beamforming is considered at each mm-wave BS because of the low implementation complexity and cost [4]. Analog beamforming results in a single communication beam that can be spatially steered towards dominant propagation path for a UE in order to serve that UE [18].

For downlink beamforming for the mm-wave tier, this paper considers that the direction of the dominant propagation path is estimated by a mm-wave BS using the uplink pilot signals transmitted by the UE [19]. The beam alignment error, ϵ, follows a truncated Gaussian distribution with a zero mean [12], [14]. The probability distribution function (PDF) of ϵ within a BS sector is written as [13]

$$f_\epsilon(y) = \frac{\sqrt{\frac{2}{\pi\sigma_\epsilon^2}}\exp\left(\frac{-y^2}{2\sigma_\epsilon^2}\right)}{\operatorname{erf}\left(\frac{\pi/3}{\sqrt{2}\sigma_\epsilon}\right) - \operatorname{erf}\left(\frac{-\pi/3}{\sqrt{2}\sigma_\epsilon}\right)}, \quad y \in \left[-\frac{\pi}{3}, \frac{\pi}{3}\right] \tag{2}$$

where σ_ϵ is the standard deviation of the beam alignment error and $\operatorname{erf}(\cdot)$ is the error function, which is defined as $\operatorname{erf}(s) = \frac{2}{\sqrt{\pi}}\int_0^z e^{-s^2} ds$. Earlier works on mm-wave beam alignment error analysis (e.g., [12], [15], [16]) considered constant values of σ_ϵ, which did not establish the dependence of ϵ on the underlying link parameters. This paper, however, adopts the approach of our recent work [13] in which σ_ϵ depends on the underlying system parameters and is obtained using the Cramér Rao lower bound (CRLB) of angle-of-arrival (AoA) estimates. With such an approach, the variance, $\sigma^2_{\epsilon_k}$, of the beam alignment error for a mm-wave link with state k is expressed as

$$\sigma^2_{\epsilon_k}(\phi, \gamma_k) = \frac{6}{\left(\frac{2\pi f_c d\cos(\phi)}{c}\right)^2 M(M^2-1)\gamma_k}, \tag{3}$$

where $k \in \{LOS, NLOS\}$, ϕ is the true AoA measured from the boresight of the array and γ_k represents the uplink received SNR of the pilot signals with channel state k at a single BS antenna element of the mm-wave BS. The parameters f_c , c, and d are the carrier frequency, the speed of light and the antenna element spacing, respectively.

The term γ_k is a function of the link length, r, and the antenna element pattern, $G_e(\phi)$. It is expressed as [13]

$$\gamma_k(\phi, r) = \frac{P_u G_e(\phi)\, \varrho_k^{ul} L_k(r)}{\sigma_s^2}, \tag{4}$$

where ϱ_k^{ul} is the channel gain experienced by the uplink pilot signals because of fading, σ_s^2 represents the noise power for the mm-wave tier and $L_k(r)$ is defined in (1). With Nakagami fading, ϱ_k^{ul} becomes a normalized gamma random variable (RV) with parameter N_k. The element pattern, $G_e(\phi)$, along the azimuth is characterized according to [20] as

$$G_{\text{e}}^{(dB)}(\phi) = G_{\max} - \min\left[12\left(\frac{\phi}{\varphi_e}\right)^2, A_m\right], \tag{5}$$

[1] In [15], directional antennas are considered for the sub-6 GHz macro-cells. However, in this paper, we consider omni-directional antennas with a 3 dBi gain for the macro-cells.

where $\phi \in \left[-\frac{\pi}{3}, \frac{\pi}{3}\right]$, $G_{\max} = 8$ dBi, $A_m = 30$ dB and $\varphi_e = 65°$ are the maximum gain, the front-to-back ratio and the half-power beamwidth (HPBW), respectively, of the single element.

To investigate the impact of mm-wave beam misalignment, it is important to characterize the array pattern in terms of the beam alignment error, ϵ. For this, we adopt the 3GPP pattern approximation, $\widetilde{G}_A(\phi, \epsilon)$, of [13] for a ULA, expressed as

$$\widetilde{G}_A(\phi, \epsilon) = \begin{cases} G_1(\phi)\, 10^{\frac{-3}{10}\left(\frac{2\epsilon}{\varphi_A}\right)^2} & \text{if } |\epsilon| \leq \Theta_A \\ G_2 & \text{if } \Theta_A \leq |\epsilon| \leq \pi, \end{cases} \tag{6}$$

where $G_1(\phi)$ and G_2 represent the values of the peak main lobe gain and the average side lobe gain, respectively. The term φ_A represents the broadside HPBW of the ULA while Θ_A is the main lobe beamwidth of the 3GPP pattern approximation corresponding to a specific value of ϕ. The parameters of $\widetilde{G}_A(\phi, \epsilon)$ are computed as follows

$$\begin{aligned} G_1(\phi) &= G_e(\phi)\ M, \qquad G_2 = \frac{1}{M \sin^2\left(\frac{3\pi}{2M}\right)}, \\ \Theta_A &= (\varphi_A/2)\sqrt{(10/3)\log_{10}\left[G_1(\phi)/G_2\right]}, \\ \varphi_A &= \pi - 2\cos^{-1}\left(\frac{1.391}{\pi M d}\right). \end{aligned} \tag{7}$$

We assume a moderate BS density and a bandwidth of the order of GHz; therefore, the mm-wave network tends to be noise-limited and is characterized by the SNR instead of the SINR [2], [5], [16]. If the typical UE is associated to the mm-wave tier, then the downlink SNR with imperfect beam alignment can be expressed as

$$SNR_s = \frac{P_s \widetilde{G}_A(\phi, \epsilon)\, \varrho_k^{dl} L_k(\|x^*\|)}{\sigma_s^2}, \tag{8}$$

where x^* is the location of the tagged BS, ϱ_k^{dl} is the channel gain due to small-scale fading with channel state k in the downlink direction, and $k \in \{LOS, NLOS\}$. For the sub-6 GHz tier, interference dominates noise and has to be accounted for. Thus, the downlink SINR is written as

$$SINR_m = \frac{P_m G_m \varrho_m^{dl} L_m(\|x^*\|)}{I_m + \sigma_m^2}, \tag{9}$$

where ϱ_m^{dl} and σ_m^2 represent the small-scale fading gain in the downlink directon and the noise power, respectively, for the sub-6 GHz tier. With Rayleigh fading, $\varrho_m^{dl} \sim \exp(1)$. The term $I_m = \sum_{x \in \Phi_m \setminus x*} P_m G_m \varrho_m^{dl} L_m(r)$ is the inter-cell interference.

We assume that the UEs are scheduled by the BSs in a round-robin manner and the resources available at a BS are shared equally among all the UEs associated to that BS. If the typical UE is associated to a mm-wave or a sub-6 GHz BS, the downlink achievable rate, $\widetilde{R}$ is obtained as [5]

$$\widetilde{R} = \begin{cases} \frac{W_s}{Q_s}\log_2(1 + SNR_s), & \text{if } x^* \in \Phi_s \\ \frac{W_m}{Q_m}\log_2(1 + SINR_m), & \text{if } x^* \in \Phi_m \end{cases} \tag{10}$$

where W_s and Q_s denote the bandwidth and the load, respectively, for the serving mm-wave BS while W_m and Q_m denote the same for the serving sub-6 GHz BS. From (8) – (10), we note that $\widetilde{R}$ is a RV.

TABLE I
NOTATION AND DEFAULT SYSTEM PARAMETER VALUES

Notation	Description	Value
λ_m, λ_s	Sub-6 GHz and mm-wave BS densities	$5/\text{km}^2$, $50/\text{km}^2$
P_m, P_s	Downlink transmit power for Sub-6 GHz and mm-wave BSs	46 dBm, 30 dBm
λ_u	UE density	$200/\text{km}^2$
P_u	UE transmit power	23 dBm
f_{c_m}, f_{c_s}	Sub-6 GHz and mm-wave carrier frequencies	2 GHz, 28 GHz
G_m	Sub-6 GHz antenna gain	3 dBi
W_m, W_s	Sub-6 GHz and mm-wave Bandwidth	20 MHz, 1 GHz
$\alpha_m, \alpha_{\text{LOS}}$, α_{NLOS}	Sub-6 GHz, mm-wave LOS and mm-wave NLOS path loss exponents, respectively	3, 2, 2.92
C_m, C_{LOS}, C_{NLOS}	Sub-6 GHz, mm-wave LOS and mm-wave NLOS path loss intercepts, respectively	-38.5 dB, -61.4 dB, -72 dB
σ_m^2	Noise power for Sub-6 GHz tier	-174 dBm/Hz + $10\log_{10}(W_1)$ + 10 dB
σ_s^2	Noise power for mm-wave tier	-174 dBm/Hz + $10\log_{10}(W_2)$ + 10 dB
$\mathcal{P}_{LOS}$, R_B	LOS ball model parameters	0.2, 200 m

The notations of different system parameters are tabulated in Table I. Unless specifically stated otherwise, the corresponding values listed in Table I are used throughout this paper.

III. Rate Coverage Probability with Conventional Cell Association

In this section, we first describe the conventional way of deciding the cell associations in a HetNet. Then, we explain the metric of rate coverage probability and illustrate how it is affected by the beam alignment errors.

A. Conventional Cell Association Strategy for HetNets

In all types of HetNets, a common and effective approach for deciding the cell associations is based on the downlink *biased* received power [5], [21]. Each tier of BSs is assigned a unique weight, known as the bias factor, which is constant within a tier [22]. A UE associates with a BS that offers the maximum downlink biased received power averaged over the small-scale fading [23]. This implies, similar to [5] and [8], that the typical UE associates with a BS located at $x^* \in \Phi_j$ only if

$$\begin{aligned} B_j P_j G_j L_j(\|x^*\|) \geq B_i P_i G_i L_{\max,i}(\|x\|), \\ \forall i, j \in \{m, s\} \end{aligned} \tag{11}$$

where $B_{(\cdot)}$ is the bias value of the corresponding tier, $L_j(\cdot)$ is defined in (1) and $L_{\max,i}(\cdot)$ represents the path-loss between the typical UE and an i^{th} tier BS that results in the maximum received power for the i^{th} tier. Recall that the path-loss for the mm-wave LOS links is different from the corresponding NLOS links. Thus, in (11), $L_j(\cdot)$ and $L_{\max,i}(\cdot)$ are defined

generally so that either of them can represent the path-loss for the mm-wave LOS links, mm-wave NLOS links and the sub-6 GHz links.

For the macro-cell tier, $B_m = 1$ is used whereas the small-cell tier employs $B_s > 1$, which helps to offload UEs from the macro-cells and corresponds to expanding the coverage region of the small-cells. Such biasing reduces the severe load imbalance across the tiers and improves the overall network performance [21]. For the mm-wave small-cell tier, maximum array gain is assumed during cell association [5], i.e., $G_s = G_1(\phi)$ and the effects of beam alignment errors are not considered during this phase [16].

B. Rate Coverage Probability in HetNets

In this subsection, we study the rate coverage probability of the HetNet with the aforementioned cell association strategy using simulations and analyze the effects of mm-wave beam alignment errors. For the simulations, 10^4 Monte-Carlo trials are conducted.

The rate coverage probability, $\mathcal{R}(\rho)$, is a metric to characterize the distribution of the achievable rate, $\widetilde{R}$, in the network. It represents the fraction of UEs whose rates are above certain predefined thresholds, ρ [4]. Mathematically, $\mathcal{R}(\rho) = \mathbb{P}[\widetilde{R} > \rho]$.

In the following, we discuss the effects of mm-wave beam alignment errors on $\mathcal{R}(\rho)$. Fig. 1 shows the trends exhibited by $\mathcal{R}(\rho)$ with imperfect and perfect alignment when the value of the bias is varied. Afterwards, Fig. 2 depicts the effects of increasing the mm-wave BS density and the number of BS antennas on $\mathcal{R}(\rho)$ with imperfect alignment.

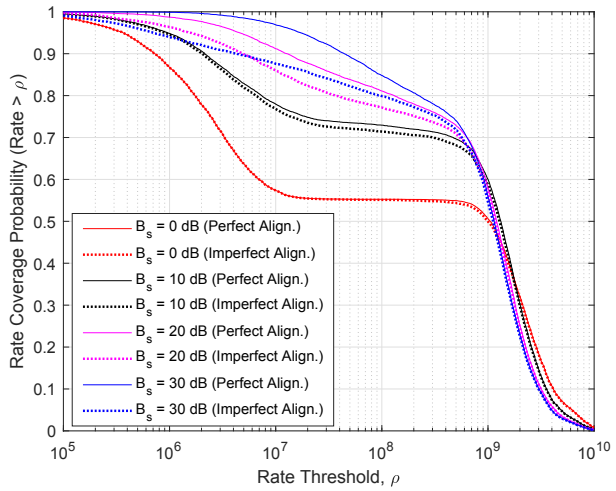

Fig. 1. Rate coverage probability with perfect and imperfect beam alignment for different bias values of the mm-wave tier. Number of BS antennas (M) for the mm-wave tier = 32, mm-wave BS density (λ_s) = $50/\text{km}^2$, sub-6 GHz BS density (λ_m) = $5/\text{km}^2$.

In Fig. 1, four different values of the bias, B_s, for the mm-wave tier are considered and the cell associations are decided according to (11). No biasing is assumed for the sub-6 GHz macro-cells. The solid curves represent the rate coverage of the HetNet with perfect alignment for the mm-wave tier while the dotted curves represent the rate coverage with imperfect alignment.

Below, we thoroughly discuss the implications on $\mathcal{R}(\rho)$ when B_s is set as 0 dB, 10 dB, 20 dB and 30 dB, respectively. We specifically show that the difference between perfect and imperfect alignment rate coverage is insignificant for $B_s = 0$ dB and $B_s = 10$ dB. However, for $B_s = 20$ dB and $B_s = 30$ dB, the difference becomes significant. Moreover, contrary to the perfect alignment scenario, the rate coverage with imperfect alignment for $B_s = 30$ dB becomes less than that for $B_s = 20$ dB for some values of ρ.

1) $B_s = 0$ dB: When $B_s = 0$ dB, i.e., no bias used for the mm-wave tier, the rate coverage with imperfect alignment is almost the same as with perfect alignment. This is because most UEs associate to the sub-6 GHz BSs in this case. The remaining UEs that associate with mm-wave BSs experience extremely good channel conditions, i.e., LOS channels, resulting in insignificant beam alignment errors [13]. Thus, the overall rate coverage does not degrade. The curve between $\rho \approx 10^7$ and $\rho = 5 \times 10^8$ is flat because of the significantly different rates provided by the sub-6 GHz and the mm-wave tiers [5]. The UEs connected to the sub-6 GHz tier experience rates less than 10^7 bits per second (bps) whereas the LOS mm-wave UEs experience rates greater than 5×10^8 bps, hence, we can quantify that approximately 55% of the UEs are connected to the LOS mm-wave BSs whereas the remaining 45% UEs are connected to the sub-6 GHz BSs.

The above observations can also be related to the LOS ball model. The value $\rho = 5 \times 10^8$ quantifies the achievable rate of the LOS mm-wave UEs at the boundary of the LOS ball. Rates lower than 5×10^8 are either due to the NLOS mm-wave channel state or the sub-6 GHz tier. Since the beam alignment errors severely affect those UEs that are served by NLOS mm-wave BSs [13], the scarcity of such UEs explains the closeness of the rate coverage probabilities with perfect and imperfect beam alignment.

2) $B_s = 10$ dB: Increasing B_s from 0 dB to 10 dB significantly increases the rate coverage probability (both with perfect and imperfect alignment) for a wide range of the rate threshold, ρ. However, the rate coverage probability for imperfect beam alignment is slightly less than that of the perfect alignment case when $10^7 < \rho < 5 \times 10^8$, although both curves follow the same trend.

The improvement, as compared to the 0 dB case, is due to both the sub-6 GHz and the mm-wave tiers. Increasing the bias offloads some UEs to the mm-wave tier, thereby reducing the load on the sub-6 GHz BSs. As a result of this offloading, more sub-6 GHz resources are made available to those UEs that are not offloaded, thus, increasing their achievable rates, as per (10). On the other hand, offloading increases the fraction of UEs associated to the mm-wave tier. Thus, on average, more UEs are able to achieve higher rates because of the huge mm-wave bandwidth. Note that in this case, almost 70% of the UEs are able to achieve an average rate of 5×10^8 bps compared to only 55% UEs when no bias was used. It is worth mentioning here that to the best of our knowledge, in the

existing works, e.g., [5] and [7], the increase in the achievable rate by offloading UEs to the mm-wave small-cells has only been attributed to the huge mm-wave bandwidth.

The difference between the perfect and the imperfect alignment rate coverage probabilities is due to those UEs that get associated to the mm-wave NLOS BSs instead of the sub-6 GHz BSs because of the 10 dB bias value. For $\rho < 10^7$, however, we observe that this difference tends to diminish and completely vanishes at a specific value of ρ. Such an observation implies that extremely low rate (i.e., less than 10^7 bps) UEs are still served by the sub-6 GHz BSs; and that a bias of 10 dB is not sufficient to offload them to the mm-wave tier and cause beam misalignment. Nevertheless, it can be inferred from these observations that a bias of 10 dB significantly improves the overall rate coverage probability of the HetNet even in the presence of mm-wave beam alignment errors. This is because the fraction of UEs that are served by NLOS mm-wave BSs is quite small in such a case.

We also notice that for $\rho \geq 2 \times 10^9$, which corresponds to the rate of mm-wave LOS UEs, $B_s = 10$ dB results in a slightly lower rate coverage than $B_s = 0$ dB. This is due to the increase of high-SNR UEs associating with mm-wave BSs, which results in an increased load, Q_s, and a decrease of the achievable rate for the mm-wave LOS UEs. For all the considered values of B_s, the beam alignment errors for the mm-wave LOS UEs are small, leading to no significant difference between perfect and imperfect alignment. Therefore, in the following discussion, we only focus on the rate coverage corresponding to the smaller values of ρ, i.e., $\rho < 5 \times 10^8$, where the effects of beam alignment errors are noticeable.

3) $B_s = 20$ dB: Increasing B_s to 20 dB further improves the rate coverage probability with perfect and imperfect beam alignment. However, a significant gap appears between the perfect and the imperfect alignment rate coverage curves.

The improvement in the rate coverage here is mainly due to the mm-wave NLOS UEs instead of the mm-wave LOS UEs. A lot of UEs, which were otherwise served by the sub-6 GHz BSs, are now served by the mm-wave NLOS BSs and the impact of mm-wave beam misalignment on the achievable rates of such UEs is substantial. However, the rate coverage with imperfect alignment for $B_s = 20$ dB is still much better than the perfect alignment rate coverage of $B_s = 10$ dB for the values of ρ under consideration. The above observations show that the use of a moderately high bias value, of the order of 20 dB, for the mm-wave tier is beneficial for the HetNet.

4) $B_s = 30$ dB: With perfect alignment, the rate coverage increases when B_s is further increased to 30 dB, for the values of ρ under discussion. However, the difference between the perfect and imperfect alignment rate coverage probabilities is quite significant for $B_s = 30$ dB as compared to other values of B_s because more UEs are offloaded to the NLOS mm-wave BSs even if the path-loss is huge. This causes significant beam alignment errors, as per (2) – (4).

More importantly, we observe that the rate coverage curves with imperfect alignment for $B_s = 30$ dB and $B_s = 20$ dB intersect each other at a point where the rate coverage is almost 90% and $\rho \approx 4 \times 10^6$. For $\rho < 4 \times 10^6$, $B_s = 20$ dB provides better rate coverage, however, $B_s = 30$ dB is more beneficial for other values of ρ. The existence of such a cross-over point shows that using a fixed bias value throughout the mm-wave tier is not the most effective approach when the beam alignment errors are accounted for.

First, let us consider in more detail the $B_s = 20$ dB and the $B_s = 30$ dB imperfect beam alignment curves on the lower-rate side of the cross-over point. We investigate the rates achieved with the two bias values at 95% coverage probability. For $B_s = 30$ dB, 95% of the UEs achieve rates of 7×10^5 bps, however, for $B_s = 20$ dB, 95% of the UEs achieve rates of 1.56×10^6 bps. Also, with $B_s = 30$ dB, the rate of 1.56×10^6 bps is achieved by 92.68% of the UEs. This implies that increasing the bias from 20 dB to 30 dB (considering $\rho = 1.56 \times 10^6$) hurts 2.32% of the lower-rate UEs as it pushes them to the mm-wave links, which suffer from excessively high beam alignment errors. This causes the UEs to achieve lower rates than they would have achieved with the sub-6 GHz tier. Additionally, we also note that at 95% coverage probability, the rate achieved with $B_s = 20$ dB is more than double the rate achieved by $B_s = 30$ dB. This is quite significant for lower-rate UEs. The above results on $B_s = 20$ dB and $B_s = 30$ dB are contrary to the claims in [5], which also studied 95% rate coverage probability (in terms of 5^{th} percentile rate) but with perfect alignment.

A similar exercise on the higher-rate side of the cross-over point in Fig. 1 shows that with $B_s = 20$ dB, 80% of the UEs achieve rates of 3.5×10^7 bps, however, the same rate is achieved by almost 83.5% of the UEs with $B_s = 30$ dB. Therefore, increasing the bias from 20 dB to 30 dB helps 3.5% of higher-rate users by pushing them to mm-wave links with low beam alignment errors. In this case, we note that at 80% coverage probability, the rate achieved with $B_s = 30$ dB is almost three times the rate achieved by $B_s = 20$ dB.

Fig. 2 shows how the rate coverage probability of the HetNet with imperfect beam alignment is impacted for the two values of B_s (i.e., 20 dB and 30 dB) when the underlying system parameters for the mm-wave tier are varied. The parameters that are varied include the number of mm-wave BS antennas, M, and the mm-wave BS density, λ_s. The pink-colored curves represent $B_s = 20$ dB while the blue-colored curves represent $B_s = 30$ dB. Two sets of curves, the solid and dashed curves, have the same M and differ in terms of λ_s. On the other hand, the dashed and dotted sets of curves have the same λ_s but differ in terms of M. The pink and blue dashed curves for $M = 32$, $\lambda_s = 50/\text{km}^2$ serve as a reference here, as they have already been explained in the context of Fig. 1.

For all the three sets of curves, we observe that the cross-over point exists between the blue and the pink curves. However, for lower-rate UEs, the gap between the two curves is wider when M and/or λ_s are smaller (e.g., $M = 32$ and $\lambda_s = 30/\text{km}^2$). Note that for $M = 128$ and $\lambda_s = 50/\text{km}^2$, the pink-colored curve is almost the same as the blue-colored curve. This trend can be explained as follows. Recall that the cross-over and the gap between the pink and blue-colored

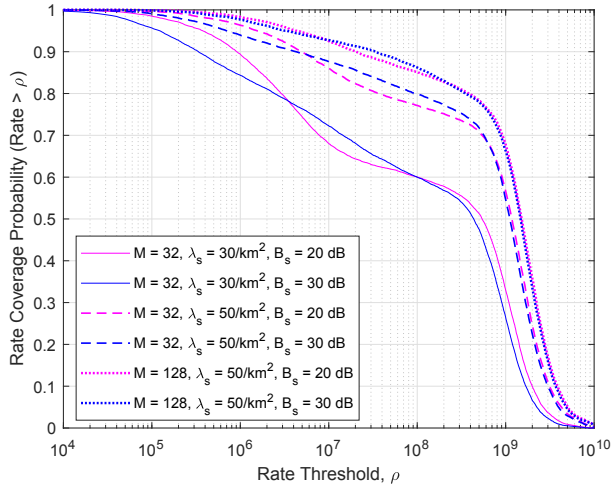

Fig. 2. Rate coverage probability with imperfect alignment for two different values of B_s. The sub-6 GHz BS density (λ_s) is fixed at 5/km^2 while the number of mm-wave BS antennas (M) and the mm-wave BS density (λ_s) are varied.

curves is due to the beam alignment errors. Increasing M lowers the variance of the beam alignment errors according to (3). This, in turn, reduces the overall effects of the alignment errors. Similarly, increasing λ_s shortens the inter-BS distance and also the UE-BS link distances for the mm-wave tier. From (3) – (4), we observe that shorter link distances result in lower variance of the beam alignment errors. From these observations, we can conclude that $B_s = 30$ dB and $B_s = 20$ dB result in almost the same rate coverage with imperfect beam alignment when M and λ_s are increased.

IV. Conclusion

This paper studies the downlink rate coverage probability of a two-tier HetNet, consisting of sub-6 GHz macro-cells and mm-wave small-cells, in the presence of mm-wave beam alignment errors, which are modeled as a function of the link path-loss. The cell associations are decided based on the conventional maximum downlink biased received power criterion. Our results indicate that with mild biasing (~ 10 dB) towards the mm-wave tier, the impact of beam alignment errors is negligible. On the other hand, aggressive biasing (~ 30 dB), while being beneficial for majority of the UEs, is actually detrimental for some UEs because it pushes them to low-rate mm-wave links with high beam alignment errors. Such UEs achieve better rates with moderate biasing (~ 20 dB). Our findings imply that extremely high biasing towards the mm-wave tier does not necessarily provide improvement when the beam alignment errors are accounted for. This discrepancy, however, can be curtailed by increasing the number of mm-wave BS antennas and/or the mm-wave BS density.

References

[1] T. S. Rappaport, G. R. MacCartney, M. K. Samimi, and S. Sun, "Wideband millimeter-wave propagation measurements and channel models for future wireless communication system design," *IEEE Trans. Commun.*, vol. 63, no. 9, pp. 3029–3056, Sep. 2015.

[2] S. Singh, M. N. Kulkarni, A. Ghosh, and J. G. Andrews, "Tractable model for rate in self-backhauled millimeter wave cellular networks," *IEEE J. Sel. Areas Commun.*, vol. 33, no. 10, pp. 2196–2211, Oct. 2015.

[3] A. Ghosh *et al.*, "Millimeter-wave enhanced local area systems: A high-data-rate approach for future wireless networks," *IEEE J. Sel. Areas Commun.*, vol. 32, no. 6, pp. 1152–1163, Jun. 2014.

[4] J. G. Andrews, T. Bai, M. N. Kulkarni, A. Alkhateeb, A. K. Gupta, and R. W. Heath, "Modeling and analyzing millimeter wave cellular systems," *IEEE Trans. Commun.*, vol. 65, no. 1, pp. 403–430, Jan. 2017.

[5] H. Elshaer, M. N. Kulkarni, F. Boccardi, J. G. Andrews, and M. Dohler, "Downlink and uplink cell association with traditional macrocells and millimeter wave small cells," *IEEE Trans. Wireless Commun.*, vol. 15, no. 9, pp. 6244–6258, Sep. 2016.

[6] M. Shi, K. Yang, C. Xing, and R. Fan, "Decoupled heterogeneous networks with millimeter wave small cells," *IEEE Trans. Wireless Commun.*, vol. 17, no. 9, pp. 5871–5884, Sep. 2018.

[7] C.-H. Liu, "Coverage-rate tradeoff analysis in mmWave heterogeneous cellular networks," *IEEE Trans. Commun.*, vol. 67, no. 2, pp. 1720–1736, Feb. 2019.

[8] Y. Shi, E. Alsusa, A. Ebrahim, and M. W. Baidas, "Uplink performance enhancement through adaptive multi-association and decoupling in UHF-mmWave hybrid networks," *IEEE Trans. Veh. Technol.*, vol. 68, no. 10, pp. 9735–9746, Oct. 2019.

[9] G. Ghatak, A. De Domenico, and M. Coupechoux, "Coverage analysis and load balancing in HetNets with millimeter wave multi-RAT small cells," *IEEE Trans. Wireless Commun.*, vol. 17, no. 5, pp. 3154–3169, May 2018.

[10] M. R. Akdeniz *et al.*, "Millimeter wave channel modeling and cellular capacity evaluation," *IEEE J. Sel. Areas Commun.*, vol. 32, no. 6, pp. 1164–1179, Jun. 2014.

[11] H. Wang, J. Fang, P. Wang, G. Yue, and H. Li, "Efficient beamforming training and channel estimation for millimeter wave OFDM systems," *IEEE Trans. Wireless Commun.*, vol. 20, no. 5, pp. 2805–2819, May 2021.

[12] M. Cheng, J. Wang, Y. Wu, X. Xia, K. Wong, and M. Lin, "Coverage analysis for millimeter wave cellular networks with imperfect beam alignment," *IEEE Trans. Veh. Technol.*, vol. 67, no. 9, pp. 8302–8314, Sep. 2018.

[13] M. S. Zia, D. M. Blough, and M. A. Weitnauer, "Effects of SNR-dependent beam alignment errors on millimeter-wave cellular networks," *IEEE Trans. Veh. Technol.*, vol. 71, no. 5, pp. 5216–5230, May 2022.

[14] A. Thornburg and R. W. Heath, "Ergodic capacity in mmWave ad hoc network with imperfect beam alignment," in *Proc. IEEE Military Commun. Conf. (MILCOM)*, Oct. 2015, pp. 1479–1484.

[15] E. Turgut and M. C. Gursoy, "Coverage in heterogeneous downlink millimeter wave cellular networks," *IEEE Trans. Commun.*, vol. 65, no. 10, pp. 4463–4477, Oct. 2017.

[16] M. Di Renzo, "Stochastic geometry modeling and analysis of multi-tier millimeter wave cellular networks," *IEEE Trans. Wireless Commun.*, vol. 14, no. 9, pp. 5038–5057, Sep. 2015.

[17] M. Haenggi, *Stochastic Geometry for Wireless Networks*. Cambridge, U.K.: Cambridge Univ. Press, 2012.

[18] R. W. Heath, N. González-Prelcic, S. Rangan, W. Roh, and A. M. Sayeed, "An overview of signal processing techniques for millimeter wave MIMO systems," *IEEE J. Sel. Topics Signal Process.*, vol. 10, no. 3, pp. 436–453, Apr. 2016.

[19] S. Kusaladharma, W. Zhu, and W. Ajib, "Stochastic geometry-based modeling and analysis of massive MIMO-enabled millimeter wave cellular networks," *IEEE Trans. Commun.*, vol. 67, no. 1, pp. 288–301, Jan. 2019.

[20] *Technical Specification Group Radio Access Network; Study of radio frequency (RF) and electromagnetic compatibility (EMC) requirements for active antenna array system (AAS) base station (Release 12)*, document 3GPP TR 37.840, 3GPP, Dec. 2013.

[21] J. G. Andrews, S. Singh, Q. Ye, X. Lin, and H. S. Dhillon, "An overview of load balancing in HetNets: Old myths and open problems," *IEEE Wireless Commun.*, vol. 21, no. 2, pp. 18–25, Apr. 2014.

[22] Y. Lin, W. Bao, W. Yu, and B. Liang, "Optimizing user association and spectrum allocation in HetNets: A utility perspective," *IEEE J. Sel. Areas Commun.*, vol. 33, no. 6, pp. 1025–1039, Jun. 2015.

[23] H.-S. Jo, Y. J. Sang, P. Xia, and J. G. Andrews, "Heterogeneous cellular networks with flexible cell association: A comprehensive downlink SINR analysis," *IEEE Trans. Wireless Commun.*, vol. 11, no. 10, pp. 3484–3495, Oct. 2012.